Local transport gap in C_{60} nanochains on a pentacene template

D. B. Dougherty,[1,*] W. Jin,[2] W. G. Cullen,[3] G. Dutton,[2] J. E. Reutt-Robey,[2] and S. W. Robey[1]
[1]*National Institute of Standards and Technology, Gaithersburg, Maryland 20899-8372, USA*
[2]*Department Chemistry and Biochemistry and Materials Research Science and Engineering Center, University of Maryland at College Park, College Park, Maryland 20742, USA*
[3]*Department of Physics and Materials Research Science and Engineering Center, University of Maryland at College Park, College Park, Maryland 20742, USA*

(Received 9 November 2007; revised manuscript received 14 December 2007; published 29 February 2008)

The adsorption of C_{60} on a bilayer film of pentacene on Ag(111) is studied with scanning tunneling microscopy and spectroscopy. At low coverage, C_{60} molecules form extended linear structures due to the templating effect of the pentacene bilayer. The C_{60} molecules in the chains adsorb at bridge sites between two neighboring pentacene molecules. The transport gap of the chain structures is measured to be 4.5 ± 0.2 eV using constant-current distance-voltage spectroscopy. The magnitude of the gap is correlated with the uniquely low coordination of the linear fullerene structures, which leads to a reduced total polarization contribution compared to bulk C_{60}.

DOI: 10.1103/PhysRevB.77.073414 PACS number(s): 73.22.−f, 68.37.Ef, 73.61.Wp

A promising approach to nanostructuring surfaces is to fabricate molecular surface assemblies that can template functional components into prescribed configurations. Beyond developing template materials and fabrication methods, it is necessary to establish correlations between real-space structure and electronic properties for both the template and the functional components. The energetic positions of electronic states are a crucial consideration for electronic device design, and controlling them through structural manipulations at the nanometer scale is technologically desirable.

Organic molecules are good candidates for carrying out templated nanostructuring of surfaces since they readily self-assemble and their interactions can be tuned by chemical functionalization. Exerting control of molecular size, shape, and interactions will translate into considerable control over the structure and function of templated molecular assemblies. Several studies (e.g., Refs. 1–7) have demonstrated the value of this approach on surfaces, focusing primarily on methods of template formation. In this Brief Report, we combine local structural and spectroscopic information that can be used to begin to develop crucial structure and/or function correlations for molecular nanostructures at surfaces.

The buckminsterfullerene molecule (C_{60}) is considered a likely building block for future nanotechnology.[8–11] Its mechanical, electrical, and chemical properties are favorable for the fabrication of reliable devices, so developing techniques for controlling nanometer-scale arrangements of fullerenes is a sought-after goal. Recently, there have been several reports of the formation of linear fullerene nanostructures on surfaces.[12–15] Interactions between C_{60} molecules tend to lead to hexagonal packing with about 1 nm spacing between molecules.[8] The formation of linear fullerene structures usually requires the use of a template such as a vicinal surface.[12,13]

In this Brief Report, we describe scanning tunneling microscopy (STM) and scanning tunneling spectroscopy (STS) observations of linear templating that results when small quantities of C_{60} are deposited onto an ordered bilayer of pentacene on Ag(111). The anisotropy that exists in the pentacene bilayer[16] supports the growth of extended linear C_{60} chains. The electronic structure of the chains is distinct from other condensed C_{60} phases[8,17] due to their linear structure. STM/STS measurements on these unique structures provide valuable insight into structure/property relations at the nanometer scale.

Experiments were carried out in an ultrahigh vacuum chamber (base pressure of $\sim 3 \times 10^{-11}$ torr) equipped with several organic molecular beam epitaxy sources and a commercial variable temperature scanning tunneling microscope (Omicron, VTSTM[18]). The Ag(111) substrate was prepared by evaporating ~300 nm of Ag onto a freshly cleaved mica surface held at approximately 500 K.[19] The resulting (111) surface was characterized by low energy electron diffraction and atomically resolved STM. Pentacene was evaporated onto the Ag(111) surface from an effusion cell [Createc SFC-40 (Ref. 18)], and the formation of an ordered bilayer was checked by STM. C_{60} was then evaporated onto the bilayer (held at room temperature) from a different effusion cell [Createc LTC-40 (Ref. 18)].

All STM imaging was carried out in constant-current mode using electrochemically etched tungsten tips. Tunneling spectroscopy was performed in constant-current distance-voltage mode. In this measurement, the tip is held above a fixed point on the surface and the feedback loop is kept active while the tip-sample bias is changed. In order to maintain constant current, the tip moves vertically relative to the surface. Resonant tunneling can be observed in tip distance-voltage ["$z(V)$"] characteristics as a sudden increase in the rate of vertical tip motion. This mode of spectroscopy has been demonstrated[20–22] to be well suited to the study of organic materials on surfaces since it can minimize the likelihood of tip-induced molecular motion or chemical reaction by maintaining a small constant current. It can also resolve local variations in electronic properties across molecular domain boundaries,[22] and it can therefore be applied to the fullerene nanostructures that are the focus of the present work.

Figure 1(a) shows an STM image of an isolated C_{60} mol-

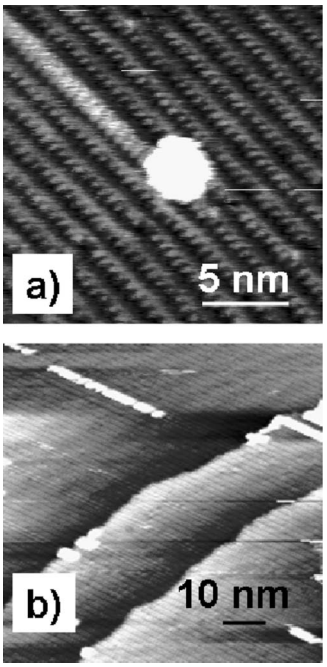

FIG. 1. (a) STM image (−0.874 V, 0.108 nA) of an isolated C_{60} molecule (apparent height of ~0.5 nm above the pentacene substrate) on the pentacene bilayer. The apparent lateral dimension of the C_{60} molecule is exaggerated due to the convolution of the real shape of the molecule with the shape of the STM tip. (b) Large-scale STM image (72.8×72.8 nm^2, −0.874 V, 0.043 nA) illustrating the formation of linear C_{60} structures on the pentacene bilayer.

ecule adsorbed on the ordered pentacene bilayer on Ag(111).[16] The pentacene bilayer displays long range order with an oblique unit cell that is highly anisotropic, giving rise to "pentacene rows" spaced by about 1.6 nm. The pentacene molecules in these rows are oriented with their long axes parallel to the plane of the substrate and their short axes tilted (by ~28°–34°) out of this plane.[16,23] At low coverage, subsequently deposited C_{60} molecules always adsorb between adjacent pentacene rows, as shown in Fig. 1(a). The observation of isolated molecules on the pentacene bilayer shows that the mobility of C_{60} on pentacene is significantly smaller than its mobility on most metals, where isolated molecules are not observed at room temperature due to rapid island formation.[8,24]

As illustrated in the STM image in Fig. 1(b), the pentacene row direction is transmitted to extended linear fullerene structures that appear as the bright lines running along the rows. The maximum length of such structures is expected to be limited primarily by the width of the terrace on which they form. The maximum (defect-free) length that we have observed is about 30 nm. These linear structures are only favored on the surface in the very low-coverage regime. When the coverage of C_{60} exceeds ~0.05 molecules/nm^2, a disordered phase (to be discussed in a separate publication) preferentially forms due to the increasing influence of lateral C_{60}-C_{60} interactions.

Figure 2 shows an STM image of a linear C_{60} structure where individual fullerene molecules can be resolved. Along the chains, molecules are separated by the typical 1.0 nm

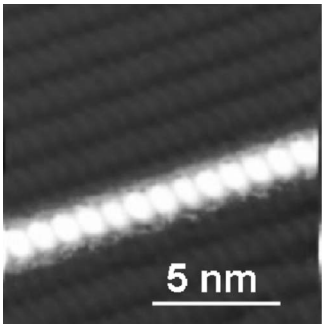

FIG. 2. STM image (12.45×12.45 nm^2, −0.456 V, 0.037 nA) showing a linear C_{60} structure. The raw image was added to a multiple of its numerical derivative to ensure that both C_{60} and pentacene molecules are clear within the color table.

spacing that is determined by C_{60}-C_{60} interactions.[8] Like the isolated C_{60} molecules, the chains are located in the trough between two pentacene rows. The highly specific interrow location of C_{60} on the pentacene bilayer is driven by intermolecular interactions between C_{60} and pentacene that include both electrostatic and dispersive contributions. A motif that is common in noncovalently bonded C_{60} complexes is the tendency for electron-rich 6-6 double bonds on the fullerene to be directed toward the most electron deficient regions of an aromatic molecule (e.g., a porphyrin[25]). Evidently, analogous electrostatic interactions contribute to the binding location of C_{60} molecules at low coverage on the pentacene bilayer since the bridge site between two pentacene rows should have a reduced electron density by comparison to the site directly on top of a pentacene molecule.

Alvarado and co-workers have shown that constant-current distance-voltage characteristics can be used to extract the transport gap $\Delta E_{\text{transport}}$ for polymer thin films.[20,21] This quantity is equal to the difference in ionization potential (IP) and electron affinity (EA) of a material and regulates the transport of externally injected charges. The local electronic structure over the pentacene bilayer and over the C_{60} chains was measured using this technique. The results serve to illustrate the impact of nanoscale environment on practical physical properties.

Figures 3(a) and 3(b) provide distance-voltage characteristics and their numerical derivatives measured for the pentacene bilayer. The differentiated spectra display resonant features near -2.0 ± 0.2 eV [average of 24 $z(V)$ sweeps] and $+1.63 \pm 0.04$ eV [average of 30 $z(V)$ sweeps] that are associated with tunneling through the pentacene highest occupied molecular orbital (HOMO) and lowest unoccupied molecular orbital (LUMO), respectively. These values yield a peak-to-peak transport gap of 3.6 ± 0.2 eV. Distance-voltage measurements performed on a nearby fullerene chain [Figs. 3(c) and 3(d)] show resonant features at -2.2 ± 0.2 eV [average of 29 $z(V)$ sweeps] and $+2.34 \pm 0.07$ eV [average of 33 $z(V)$ sweeps], yielding a transport gap of 4.5 ± 0.2 eV. The error bars in all measurements are taken as the standard deviation of repeated measurements of the peak positions in the numerical derivatives of distance-voltage characteristics for different points in the bilayer or different points along the C_{60} chain.

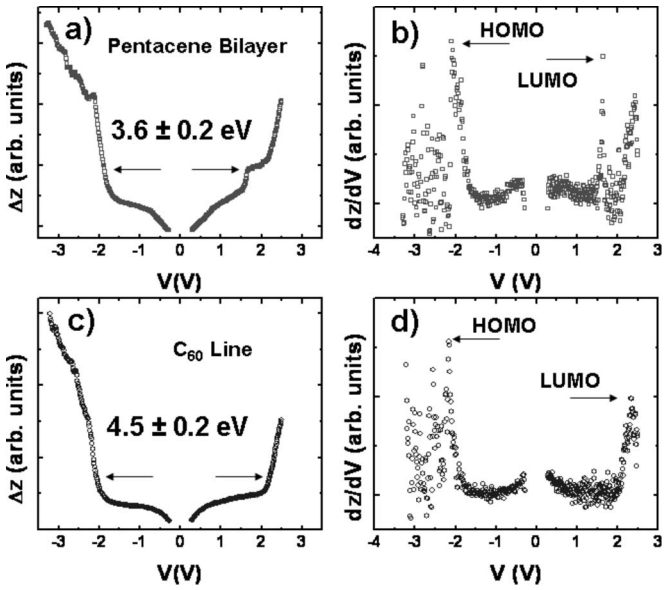

FIG. 3. (a) Constant-current distance-voltage characteristics (+1.2 V, 0.023 nA) measured on the pentacene bilayer. (b) Numerical derivative of the data in part (a) with HOMO and LUMO peak postions indicated. (c) Constant-current distance-voltage characteristics (+1.2 V, 0.023 nA) measured locally on a C_{60} line. (d) Numerical derivative of the data in part (c).

Distance-voltage characteristics obtained for C_{60} chains with lengths ranging from 10 to 30 nm yielded no significant differences. All chains were lengthwise sampled to within 3 nm (approximately three C_{60} molecules) of the chain ends. Shorter chains and chain ends were not sampled to preserve the stability of the tunneling junctions for spectroscopy. Measurements performed with different tunneling tips, pentacene films, and C_{60} chains yielded values comparable to those illustrated in Fig. 3.

In a solid state molecular system, the transport gap may be understood as the difference between the IP and EA of the isolated molecule in the *gas phase* reduced by a polarization energy E_{pol}, which arises from the response of charge densities in neighboring molecules to electron addition or removal.[26,27] This polarization response stabilizes injected electrons or holes, resulting in a reduced gap between $N+1$ electron and $N-1$ electron states in the solid compared to its gas phase value.[27] The amount of stabilization depends on details of the local environment such as the polarizability and the number of near-neighbor molecules.

With this in mind, we can rationalize the spectroscopic measurements presented in Fig. 3 on the basis of the local environments of the pentacene bilayer and the linear C_{60} structures. As a start, we consider the pentacene bilayer for which the measured gap [Fig. 3(a)] is essentially the same as the 3.42 eV (peak-to-peak) transport gap measured for a thick pentacene films on Au surfaces.[28] This implies that the pentacene bilayer is thick enough to provide significant electrical decoupling of the templated C_{60} chain structures from the Ag(111) surface. As a side note, the correspondence between the electronic properties of the pentacene bilayer measured here and those of very thick pentacene films[28] provides supporting evidence for its assignment as a true second layer.[16,23]

In contrast to the observation of a bulklike transport gap for the pentacene bilayer, the magnitude of the gap measured for the C_{60} chain structures more closely resembles the gas phase value [IP-EA=4.9 eV (Ref. 17)] than the value for thick C_{60} films [$\Delta E_{transport}$=3.7 eV (Ref. 17)]. The C_{60} HOMO is shifted away from the Fermi level by ~0.2 eV and the C_{60} LUMO is shifted away from the Fermi level by ~0.6 eV when compared to a bulk fullerene crystal.[17] We attribute these differences to the reduced coordination of the molecules in the linear fullerene structures, which reduces the total polarization response of the surroundings of the chain when electrons are added or removed.

This interpretation can be semiquantitatively justified by neglecting the polarization response of the pentacene bilayer on which the C_{60} chains are grown and by treating them as isolated objects. One can then track an approximately linear increase in polarization energy versus the number of C_{60} near neighbors (NNs). The polarization energy increases from 0 eV in the gas phase [0 NN IP-EA=4.9 eV (Ref. 17)] to 0.4 ± 0.2 eV for the linear structures described here (2 NN, $\Delta E_{transport}=4.5 \pm 0.2$ eV) to ~1.2 eV for the surface of bulk C_{60} [9 NN, $\Delta E_{transport}$=3.7 eV (Ref. 17)]. From a linear fit to polarization energy versus number of NNs[8] (assuming an ~0.1 eV uncertainty in the polarization energies extracted from Ref. 17), it is estimated that each near-neighbor C_{60} molecule in a solid state system adds 0.13 ± 0.02 eV/NN polarization stabilization to the transport gap.

Simple electrostatic considerations allow an estimate of the expected total polarization energy in C_{60} solids using the formula $E_{pol}=(ze^2\alpha/R^4)$, where z is the number of NN molecules, α is the molecular polarizability [~0.085 nm^3 (Ref. 8)], and R is the NN spacing of ~1.0 nm. The value of 0.12 eV/NN (Ref. 8) obtained from this formula is in good agreement with the estimate from the linear fit mentioned above. Naturally, the pentacene molecules underneath the chains will add polarization stabilization in addition to this C_{60} contribution. We obtain acceptable agreement with the rough electrostatic calculation, despite neglecting this contribution, because the magnitude of the total polarization energy associated with the pentacene film will most likely be less than or comparable to the experimental uncertainty in our determination of the transport gap.

These considerations also assume an equal polarization contribution from both the HOMO and the LUMO. This is not the case in our experiments where the LUMO is more significantly altered (relative to bulk C_{60}) by the reduced coordination than the HOMO. A more complete treatment would need to determine the polarization energy for electrons and holes separately in addition to considering the polarization response of the pentacene bilayer on which C_{60} chains are supported. However, given the agreement between the electrostatic arguments above and the experimental polarization energies, it is clear that the major contributor to the magnitude of the measured transport gap is the low coordination of the C_{60} molecules in the chains.

In summary, we have described the formation of linear C_{60} structures resulting from the adsorption of C_{60} on an

anisotropic pentacene bilayer template. At low coverage, C_{60} molecules occupy spaces in troughs between parallel rows of pentacene molecules and form chains with bulklike C_{60}-C_{60} spacings. The transport gap measured locally for the linear C_{60} chains is 4.5 ± 0.2 eV. This value is much higher than the corresponding gap for bulk C_{60} due to the reduced coordination of the linear configuration that lowers the overall polarization energy upon electron addition or removal. These measurements provide direct evidence for the crucial role of local environment in determining functional properties in nanometer-scale systems.

We acknowledge useful discussions with L. J. Richter, Y.-J. Song, and J. Crain. This work was supported by the Department of Commerce through the NIST Center of Nanomanufacturing and Metrology and the NSF-funded MRSEC via No. DMR-05-20471. Use of the UHV microscopy facilities is supported by the University of Maryland, NSF-MRSEC.

*Corresponding author. dan.dougherty@nist.gov

[1] F. Rosei, M. Schunack, P. Jiang, A. Gourdon, E. Laegsgaard, I. Stensgaard, C. Joachim, and F. Besenbacher, Science **296**, 328 (2002).
[2] J. V. Barth, G. Constantini, and K. Kern, Nature (London) **437**, 671 (2005).
[3] E. Mena-Osteritz and P. Bauerle, Adv. Mater. (Weinheim, Ger.) **18**, 447 (2006).
[4] A. Kiebele, D. Bonifazi, F. Cheng, M. Stöhr, F. Diederich, T. Jung, and H. Spillmann, ChemPhysChem **7**, 1462 (2006).
[5] D. Bonifazi, A. Kiebele, M. Stöhr, F. Cheng, T. Jung, F. Diederich, and H. Spillmann, Adv. Funct. Mater. **17**, 1051 (2007).
[6] N. Wintjes, D. Bonifazi, F. Cheng, A. Kiebele, M. Stöhr, T. Jung, H. Spillmann, and F. Diederich, Angew. Chem., Int. Ed. **46**, 4089 (2007).
[7] B. Xu, C. Tao, W. G. Cullen, J. E. Reutt-Robey, and E. D. Williams, Nano Lett. **5**, 2207 (2005).
[8] M. S. Dresselhaus, G. Dresselhaus, and P. C. Ecklund, *Science of Fullerenes and Carbon Nanotubes* (Academic, San Diego, 1996).
[9] C. Joachim and J. Gimzewski, Chem. Phys. Lett. **265**, 353 (1997).
[10] P. Moriarty, Rep. Prog. Phys. **64**, 297 (2001).
[11] D. M. Guldi, F. Zerbbetto, V. Georgakilas, and M. Prato, Acc. Chem. Res. **38**, 38 (2005).
[12] W. Xiao, P. Ruffieux, A.-M. Kamel, O. Gröning, K. Palotas, W. A. Hofer, P. Gröning, and R. Fasel, J. Phys. Chem. B **110**, 21394 (2006).
[13] N. Néel, J. Kröger, and R. Berndt, Adv. Mater. (Weinheim, Ger.) **18**, 174 (2006).
[14] S. K. Klitgaard, K. Egeblad, L. T. Haahr, M. K. Hansen, D. Hansen, J. Svagin, and C. H. Christensen, Surf. Sci. **601**, L35 (2007).
[15] M. Feng, J. Lee, J. Zhao, H. Petek, and J. T. Yates, Jr., J. Am. Chem. Soc. **129**, 12394 (2007).
[16] M. Eremtchenko, R. Temirov, D. Bauer, J. A. Schaefer, and F. S. Tautz, Phys. Rev. B **72**, 115430 (2005).
[17] T. R. Ohno, Y. Chen, S. E. Harvey, G. H. Kroll, J. H. Weaver, R. E. Haufler, and R. E. Smalley, Phys. Rev. B **44**, 13747 (1991).
[18] Certain commercial equipment, instruments, or materials are identified in this Brief Report to foster understanding. Such identification does not imply recommendation by the National Institute of Standards and Technology, nor does it imply that the materials or equipment identified are necessarily the best available for this purpose.
[19] A. A. Baski and H. Fuchs, Surf. Sci. **313**, 275 (1994).
[20] S. F. Alvarado, P. F. Seidler, D. G. Lidzey, and D. D. C. Bradley, Phys. Rev. Lett. **81**, 1082 (1998).
[21] M. Kemerink, S. F. Alvarado, P. Müller, P. M. Koenraad, H. W. M. Salemink, J. H. Wolter, and R. A. J. Janssen, Phys. Rev. B **70**, 045202 (2004).
[22] D. B. Dougherty, P. Maksymovych, J. Lee, and J. T. Yates, Jr., Phys. Rev. Lett. **97**, 236806 (2006).
[23] D. Käfer and G. Witte, Chem. Phys. Lett. **442**, 376 (2007).
[24] E. I. Altman and R. J. Colton, Phys. Rev. B **48**, 18244 (1993).
[25] M. J. Shephard and M. N. Paddon-Row, J. Porphyrins Phthalocyanines **6**, 783 (2002).
[26] M. Schwoerer and H. C. Wolf, *Organic Molecular Solids* (Wiley-VCH, Weinheim, 2007), Chap. 8.
[27] E. V. Tsiper and Z. G. Soos, Phys. Rev. B **64**, 195124 (2001).
[28] F. Amy, C. Chan, and A. Kahn, Org. Electron. **6**, 85 (2005).